The noise performance of electron-multiplying charge-coupled devices at soft X-ray energy values

The Noise Performance of Electron Multiplying Charge-Coupled Devices at soft X-ray energies

James H. Tutt, Andrew D. Holland, Neil J. Murray, David J. Hall, Richard D. Harriss, Andrew Clarke, Anthony M. Evagora

***Abstract*—The use of EM-CCDs for high resolution soft X-ray spectroscopy has been proposed in previous studies and the analysis that followed identified and verified experimentally a Modified Fano Factor for X-ray detection using an ^{55}Fe X-ray source. However, further experiments with soft X-rays at 1000 eV were less successful, attributed to excessive split events. More recently, through the use of a deep depletion e2v CCD220 and on-chip binning, it was possible to greatly reduce the number of split events allowing the result for the Modified Fano Factor at soft X-ray energies to be verified. This paper looks at the earlier attempt to verify the Modified Fano Factor at 1000 eV with a e2v CCD97 and shows the issues created by the splitting of the charge cloud between pixels. It then compares these earlier results with new data collected using the e2v CCD220, investigating how split event reduction allows the Modified Fano Factor to be verified for low energy X-rays.**

***Index Terms*—CCD, EM-CCD, Excess Noise factor, Fano factor, X-ray, Modified Fano Factor**

I. Introduction

CCDs have been used in several X-ray applications as they offer inherent energy and spatial resolution with a high Quantum Efficiency. The drive has been towards creating a CCD with very low levels of readout noise. The Electron-Multiplying CCD has made this possible through the use of impact ionisation to increase the number of electrons in the charge packet before the signal is read out, thereby suppressing the readout noise and increasing the Signal-to-Noise Ratio (SNR) [1]. The gain, G, is dependent on the potential on the gate electrodes in the multiplication register and the number of gain elements, N, that the charge packet passes through [2]. An increase in the potential on the gate electrode causes an increase in the probability of additional electrons being generated and this can be quantified as a gain per stage, g. The total gain through the N stages is therefore given by:

$$G = (1+g)^N \tag{1}$$

The gain process is advantageous in situations where small signals are being detected in a low flux photon environment, such as photon counting at soft X-ray energies. However, the stochastic nature of multiplication gain adds another component of noise. This noise is analogous to shot noise as it is dependent on the number of electrons in the charge packet, but it is also dependent on the amount of gain. This increase in noise has been analysed at optical photon energies and can be described by the Excess Noise Factor, F [3], and with 5898 eV X-rays from ^{55}Fe where it is described by the Modified Fano Factor, F_{mod} [1]. The result at lower X-ray energies was expected to follow the same result that was achieved at 5898 eV and was predicted through a Monte Carlo simulation and analytically [1]. This paper looks at the results of two experiments using 1000 eV X-rays from the PTB beamline (Physikalisch-Technische Bundesanstalt) at BESSY II. The first experiment with the CCD97 failed to verify the Modified Fano Factor due to incomplete charge collection caused by the electrons being split between several pixels (split events), but the second experiment with the CCD220 was tailored to minimise split events and lead to the verification of the Modified Fano Factor at 1000 eV.

The authors are with the Centre for Electronic Imaging, Planetary Space Sciences Research Institute, The Open University, Milton Keynes, UK.

II. The EM-CCDs used for the verification for the Modified Fano Factor at 1000 eV

This section describes the two devices used for the experiments at the PTB beamline, particularly focusing on the e2v CCD220 used in the second experiment and how it is able to minimise split events.

A. e2v CCD97

The CCD97 used in this study, shown in Figure 1, is a frame transfer EM-CCD with an image section of 512 pixels $\times$ 512 pixels that are 16 μm square. The multiplication register contains 536 gain elements. The chip is back-illuminated and has no anti-reflection coating in order to maximise its soft X-ray detection quantum efficiency [4]. The silicon has been thinned to 14 μm$\pm$1 μm. The depletion depth is 3 μm$\pm$1 μm (this can be calculated from Equation 2) and so the total field-free region is $\sim$11 μm.

B. e2v CCD220

The CCD220, shown in Figure 2, is a split frame transfer EM-CCD with the readout further split into 8 separate sections. This splitting allows the device to be read out more quickly and thereby minimises the dark signal that is collected [5]. The image area is 240 pixels x 240 pixels that are 24 μm square and each multiplication register contains 520 gain elements. The chip is back-illuminated and supplied with an anti-reflection coating of hafnium oxide that optimises the device's performance with optical inputs. This reduces the quantum efficiency of the EM-CCD at very soft X-ray energies, but should not have affected the required measurements in this experiment. The device is mounted in a package with a TEC cooler and has 8 outputs.

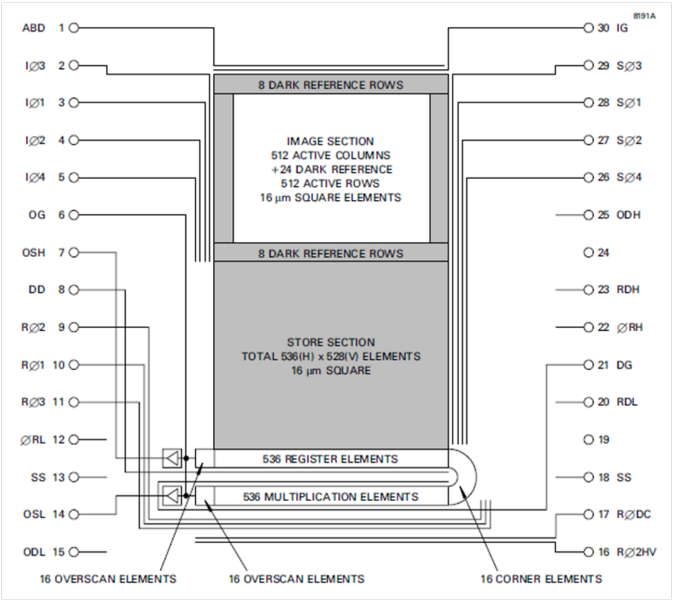

(a) Device schematic [4].

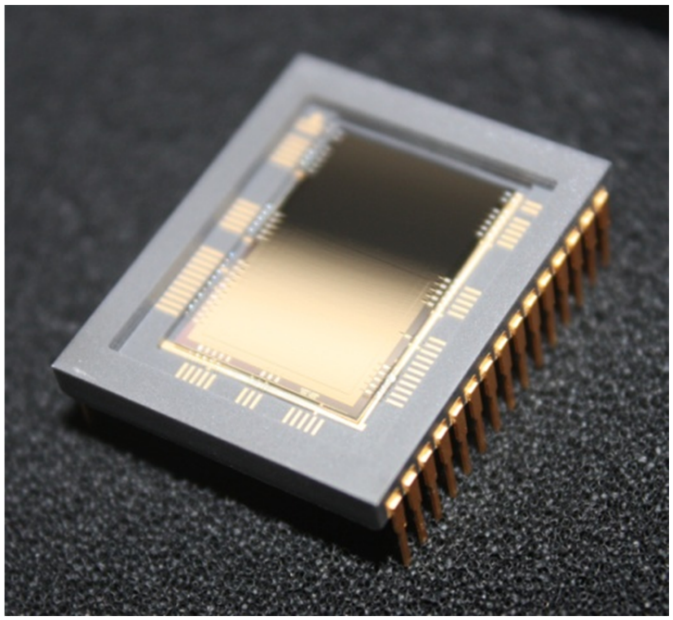

(b) Photograph of device.

Fig. 1. The e2v CCD97 used in the original experiment at BESSY II.

C. Considerations of depletion depth

The depletion depth from the surface, x_d, in a device can be found using Equation 2 [6], where ϵ_{Si} is the permittivity of silicon, V_{AVG} is the average depletion driving potential, V_{SS} is the substrate potential, q is the electronic charge and N_A is the silicon acceptor dopant concentration.

$$x_d\,(\mu m) = 1000\sqrt{\frac{2\epsilon_{Si}\,(V_{AVG} - V_{SS})}{qN_A}} \qquad (2)$$

Equation 2 shows that the depletion in a CCD can be increased by reducing the doping concentration in the silicon or by increasing the average driving potential. Conventionally an EM-CCD is manufactured on a low resistivity material as devices manufactured on higher resistivity silicon have been found to require much higher potentials to achieve the same gain values [7].

The CCD97 is manufactured on 20 Ωcm bulk silicon with equates to a dopant concentration of $\approx 5 \times 10^{14}$ cm^{-3} and a depletion depth of $\sim$3 μm (as mentioned in Section II A). To fully deplete a CCD the resistivity of the silicon needs to be higher, but this can be too high to make an effective EM-CCD.

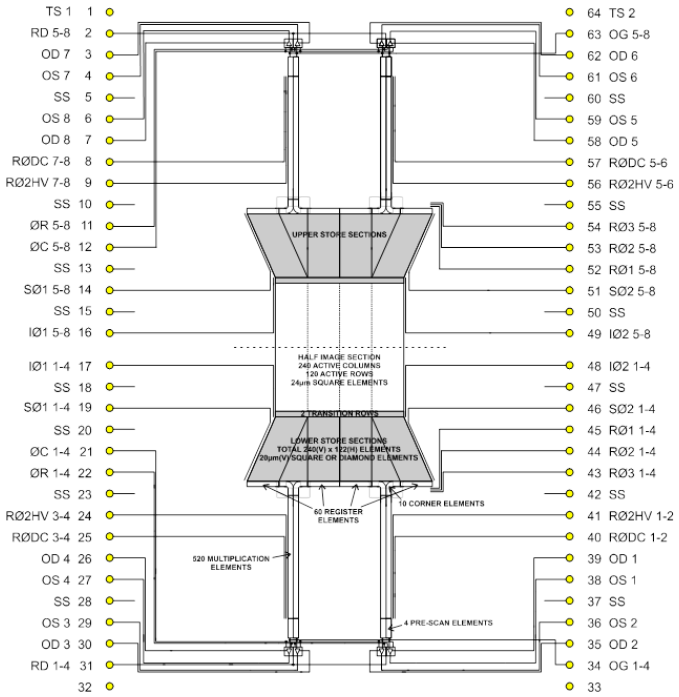

(a) Schematic of e2v CCD220 [5].

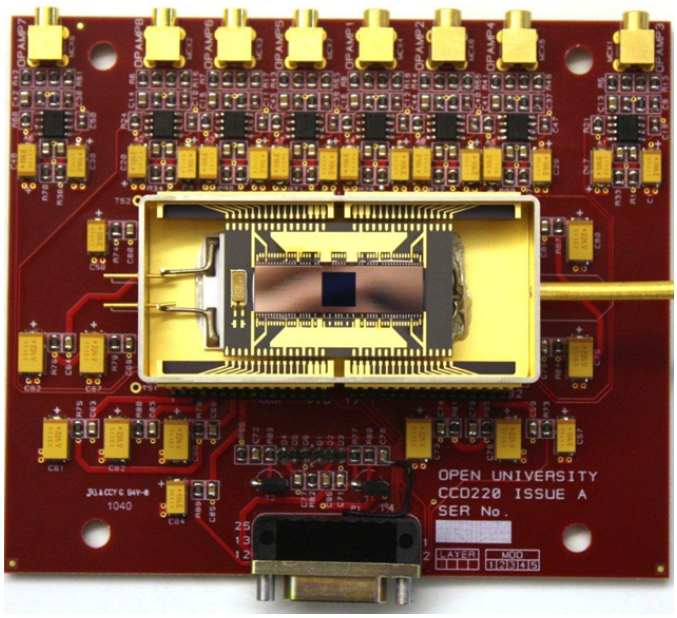

(b) Photo of the e2v CCD220.

Fig. 2. The schematic of the e2v CCD220 used in the second experiment at BESSY II (Figure 2(a)) and a picture of the device used mounted on a headboard (Figure 2(b)).

The CCD220 is a CCD with an integrated electronic shutter [8], but without the shutter drain implant. The lack of the

shutter drain means that the device has no electronic shutter capability, but the device is read out quickly in frame transfer mode making an electronic shutter unnecessary. In order to manufacture a deep depletion EM-CCD a p-well is included in the silicon to cater for the high resistivity deep depletion and low resistivity EM-CCD aspects of the device. This p-well constricts the depleted region of the EM-CCD, under normal clocking conditions to a depth close to the front surface where the resistivity is a few Ωcm. During integration, however, the clocks can have a higher potential and the depletion region can then punch through the p-well and into the higher resistivity silicon (1500 Ωcm) allowing the device to deplete further. The profile of the doping is shown in Figure 3.

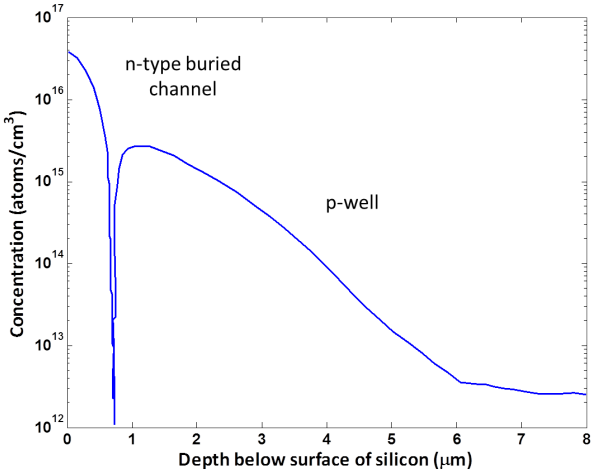

Fig. 3. The doping profile of the CCD220 differs from a normal CCD with the inclusion of the p-well doping to act as a barrier between the high and low resistivity silicon [9].

Using the Poisson equation it is possible to turn this doping profile into a potential profile for different gate potentials. This was achieved using the SILVACO TCAD programme and the result is shown in Figure 4.

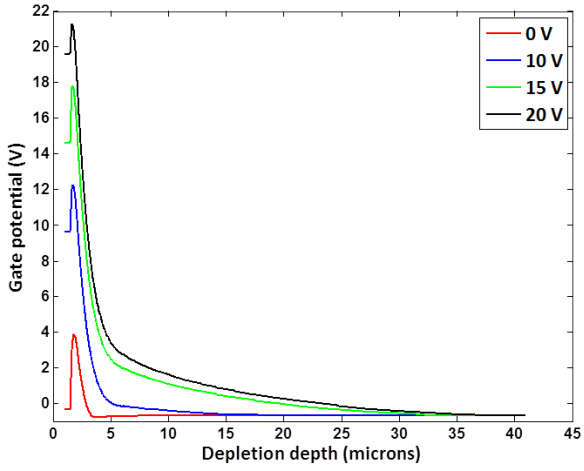

Fig. 4. The potential profile in the CCD220 for different gate voltages is shown.

The CCD220 is ∼40 μm thick and is clocked with 11 V on the image and store electrodes. This means that during normal clocking the depleted depth in the silicon is ∼15 μm; however, during integration the EM-CCD has both of its image clocks held at 17 V. This now equates to a depletion depth of ∼35 μm, almost fully depleting the device. The amount of event splitting that occurs in the device is dependent on the time it takes for the generated electrons to be collected in the buried channel. If the device is fully depleted, the collection time is small, reducing the spread of the charge packet and reducing the number of split events. Split events were determined to be the cause of the poor results from the initial experiment with the CCD97 discussed in [10], therefore the reduction of this effect during the second experiment was a high priority. The CCD220 has larger pixels than the CCD97, which helps to reduce the number of split events by having a large area per pixel for the charge cloud to be collected in.

III. Charge Spreading in Field-Free Silicon

When charge is generated in undepleted silicon it diffuses isotropically towards the depleted silicon. This leads to an increase in charge cloud size (FWHM) that, to a first approximation, is equal to twice the distance of field-free silicon that the generated charge has to travel though before it enters depletion, D, as shown in Figure 5 [11]. The size of the charge cloud created by the initial interaction is small compared to the pixel size of the devices and the diffusion that occurs in the field-free region, and so it is not considered in the split event minimisation strategy [12].

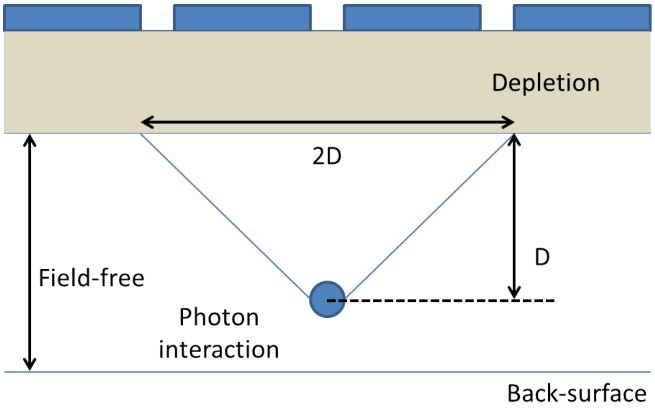

Fig. 5. The FWHM of the charge cloud generated by the photon interaction is approximately equal to twice the distance that the cloud has to travel though the field-free region of silicon.

In the original experiment at BESSY II with the CCD97 and 1000 eV X-rays, the charge was collected in 2x2 binned pixels. The effect of the X-ray interaction position on the amount of charge splitting is shown in Figure 6.

The CCD220, when integrated with clocks held at 17 V, has a field-free region of ∼5 μm. This leads to a FWHM of the electron charge cloud of ∼10 μm. The CCD220 was binned asymmetrically making the pixels 72 μm x 42 μm increasing the probability of all of the charge from a photon interaction being collected in one pixel.

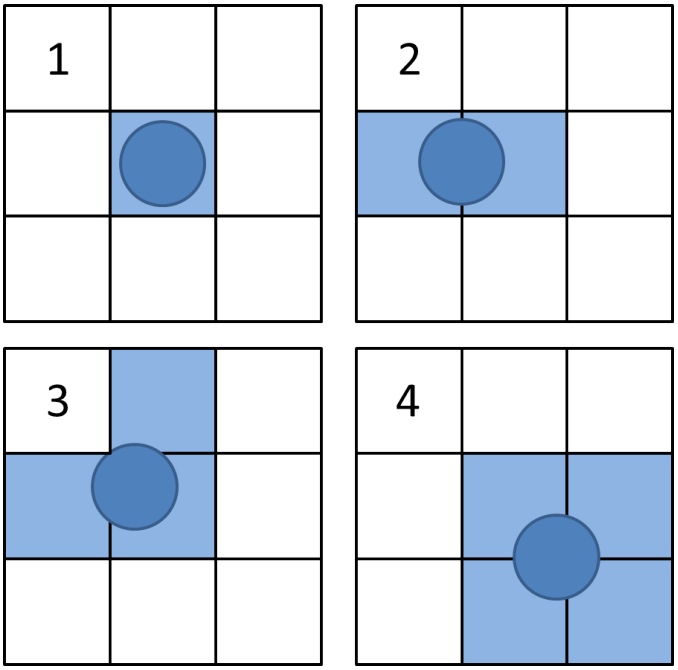

Fig. 6. X-ray interactions underneath the centre of the pixel lead to the charge cloud being completely collected in the pixel (1). Interactions towards the edges of the pixel cause the charge to be split between pixels (2-4). The amount of charge in each pixel is dependent on the interaction position.

IV. Experimental Method

The experiments for both of the devices were completed in the same way. The EM-CCD was mounted on a copper cold finger in a vacuum chamber (Figure 7).

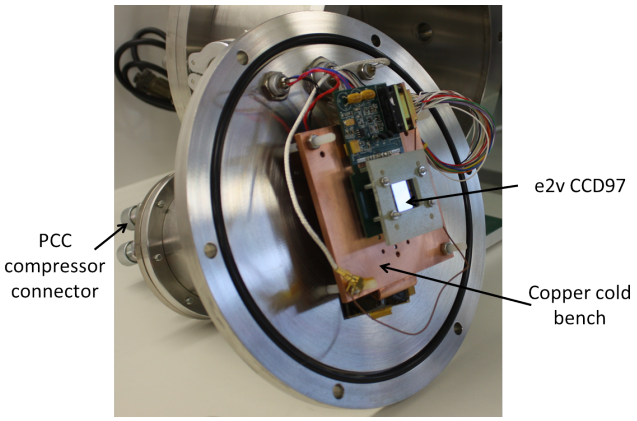

Fig. 7. The e2v CCD97 is shown mounted on a copper cold bench to provide cooing and on a vacuum chamber flange so that the experiment can be performed under vacuum.

The cooling for the device was supplied using a PCC compressor and Cryo-tiger head from MegaTech ltd. The CCD97 was cooled to -120° C to suppress the dark current generated by the device to a negligible level [10], but the CCD220 was cooled to only -50° C (the minimum possible with the available equipment). As a result there was still some dark current generation that has to be accounted for in the data analysis. This is especially true at higher levels of gain as the multiplication process will cause an increase in the dark current generated signal as well as the X-ray photon signal. The expected dark current generation is shown in Figure 8. Creating larger pixels through binning causes an increase in the dark signal collected per binned pixel and at -50° C the CCD220 had 0.04 electrons generated per binned pixel per second. The CCD97 at -120° C had a negligible dark signal of the order 10^{-11} electrons per pixel per second.

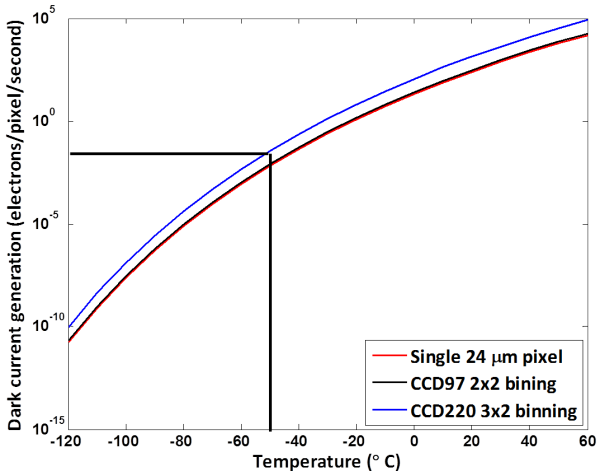

Fig. 8. Dark current generation (electrons per pixel per second) is shown for a single pixel of 24 μm along with the generation for the e2v CC97 with 2x2 binning and the CCD220 with 3x2 binning. The operating temperature of the e2v CCD220 during the experiment (-50° C) is marked [4]

Avalanche gain is temperature dependant [13] making it important to keep the temperature of the EM-CCD constant. The potential was varied from 20 V (taken as G = 1) up to the voltage where the 16-bit ADC of the readout electronics becomes saturated. The FWHM of the detected X-rays and noise peak could then be measured and Equation 3 used to calculated the value for the Modified Fano Factor, F_{mod}, at that level of gain, G [14]. The FWHM is in eV and all noise quantities are measured in electrons.

$$F_{mod} = \left(\frac{FWHM^2}{(2.355\omega)^2} - \left(\frac{\sigma_{readout}}{G} \right)^2 - F_{dark}^2 \sigma_{dark}^2 \right) \left(\frac{\omega}{E} \right) \tag{3}$$

Fitting a Gaussian to the X-ray peak and the noise peak allowed the FWHM and $\sigma_{readout}$ to be found respectively. The CCD97 was run cold enough to sufficiently suppress the dark current making $\sigma_{dark} \approx 0$, but as the CCD220 device was warmer, the dark current must be taken into account. The contribution from the dark current can be calculated by simply looking at the background level of the image and the overscan regions. Figure 9 shows the raw spectrum from an image taken at a gain of 10 where the overscan and image background peaks are clearly visible. These can be looked at separately to calculate their noise contribution.

The overscan background peak shows the contribution of noise from the readout of the device, $\sigma_{readout}$ and the background from the image area will give the combined readout and dark current noise, $\sigma_{combined}$. As errors add in quadrature, the noise on the dark current is given by:

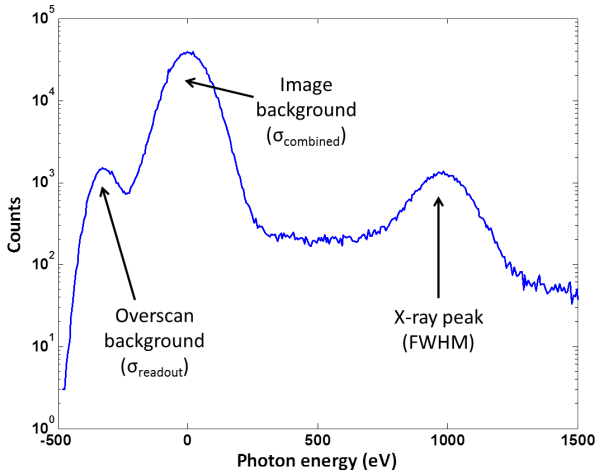

Fig. 9. The signal levels of the overscan and image are clearly visible in this spectrum. Looking at each area in isolation allows the peaks to be fitted and the contribution to the noise of the readout and the dark current can be found.

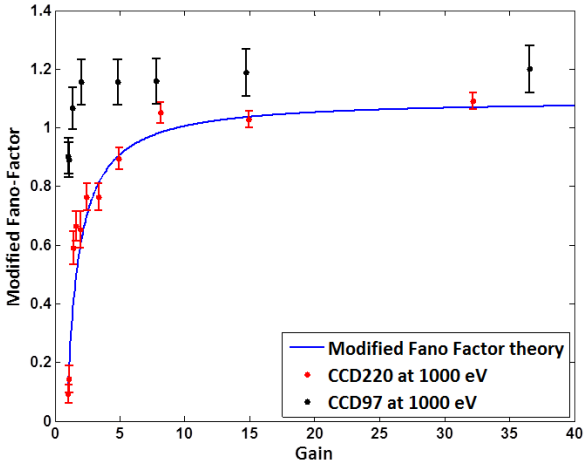

Fig. 10. A comparison between the results for the Modified Fano Factor from the e2v CCD97 and e2v CCD220.

$$\sigma_{dark} = \sqrt{(\sigma^2_{combined} - \sigma^2_{readout})} \tag{4}$$

The noise on the image background peak is a combination of the dark current and readout noise and so is sufficient for the calculation of F_{mod}. The effect of the gain on the signal is also taken into account through the measurement of the FWHM and therefore for the CCD220, the Modified Fano Factor becomes:

$$F_{mod} = \left(\frac{FWHM^2}{(2.355\omega)^2} - \sigma^2_{combined}\right)\left(\frac{\omega}{E}\right) \tag{5}$$

V. Result

The results from the CCD97 experiment are discussed in [10] and are shown by the black points in Figure 10. The red points show the results from the CCD220 measurement taken at BESSY II and the blue line is the result predicted from the theory discussed in [1].

Work completed in the laboratory allowed the Modified Fano Factor for X-rays at aluminium K-shell fluorescence (1487 eV) energy to be investigated, Figure 11.

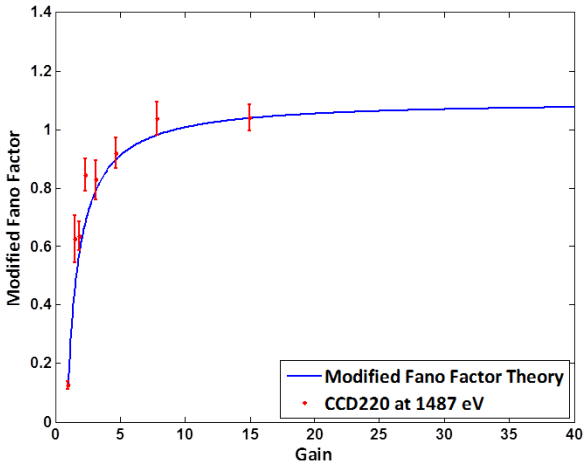

Fig. 11. Results for the Modified Fano factor at Al K-shell emission (1487 eV).

VI. Discussion

A. X-ray damage in CCDs

The interaction of highly energetic X-ray photons on silicon can produce permanent changes in the device, especially if the interaction occurs in the oxide layers that surround the electrode structure though the creation of traps in the oxide layer [15]. The X-ray damage caused by the X-rays manifests itself in four ways: 1) An increase in dark current from the Si-SiO_2 interface, 2) The oxide becomes charged causing a voltage shift in the operating biases, 3) Charge Transfer Efficiency (CTE) degradation, 4) Trap formation [16]. In this experiment, a substantial increase in the dark current over the course of the experiment would lead to an increase in the noise on the system and could affect the result; therefore, the effect must be considered. If a device is run in inverted mode, the increase in dark current can be suppressed, but in this experiment the device was run non-inverted [17].

It has been shown that, in a Front-illuminated device, radiation damage effects occurs after $\approx 10^5$ rad [18] and this experiment to investigate the Modified Fano Factor was conducted at a low X-ray flux level to allow photon counting (10,000 X-rays per gain level). Over the course of the experiment an insufficient number of X-rays were incident onto the CCD to achieve the necessary level of radiation damage to cause any effects discussed above. Soft X-ray radiation damage effects are also more prominent in front-illuminated devices as the Si-SiO_2 interface is closer to the device surface; therefore, the back-illuminated CCDs used in this experiment would require an even high flux to have a large increase in dark current [19].

B. Generation/recombination centre charge loss

Charge that is generated close to the surface of a back-illuminated CCD by the interaction of a low energy X-ray can be lost to the generation/recombination centres present [20], especially if the device is not deep-depleted and the generated electrons can drift in a field-free region [21]. The resulting partial event would affect the value found for the Modified Fano Factor. In this experiment, the device was operated at an integration potential that caused the depletion to be driven towards the back surface of the CCD minimising charge loss, Figure 4. To investigate this effect, the integration voltage on the CCD was varied from normal clocking voltages (10 V) to the integration voltage used in the experiment (17 V). By measuring the position of the the X-ray peak at each voltage the charge loss could be estimated. If signal is lost from the charge cloud, the position of the peak would be at a lower energy than would be expected. The energy scale is calibrated at using the X-ray peak position with an integration voltage of 17 V. The result of this investigation is shown in Figure 12

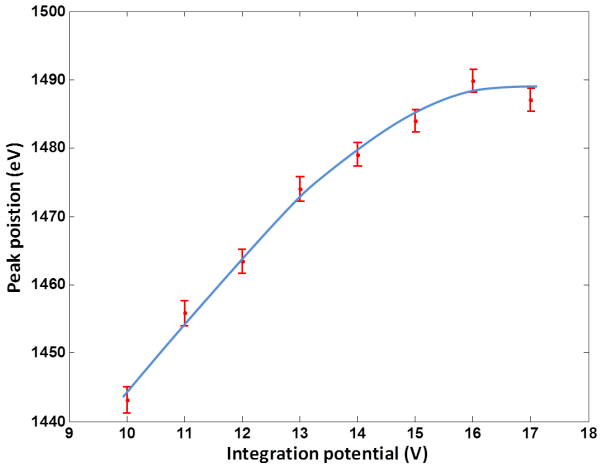

Fig. 12. The calibrated X-ray peak position from increasing integration voltage for 1487 eV. The energy scale is calibrated at using the X-ray peak position with an integration voltage of 17 V.

The result shows that when the depletion is not driven to the back-surface, charge is lost to the generation/recombination centres resulting in a fall in the X-ray peak position; however, at the integration voltage used in this experiment the curve is flattening off suggesting that the depletion stretches to the back-surface and charge loss in minimised. During the experiment the integration voltage was kept constant and so charge loss to the centres would be equal across all of the measurements. A constant experimental method and large integration voltage enables the charged loss effect to be mitigated.

VII. Conclusion

The results from the CCD220 are in very good agreement with the theoretical value for the Modified Fano Factor. The results show that when the device is deep-depleted and the pixels are made larger using on-chip binning, the effect of multiplication gain is consistent with that predicted by theory. The new result for the Modified Fano Factor suggests that the initial experiment did not verify the Modified Fano Factor due to the amount of charge splitting in the device, making an accurate value for the FWHM of the X-ray peak difficult to determine. The experiment conducted in the laboratory was also able to show that the Modified Fano Factor was correct at 1487 eV through the fluorescence of the Al K-shell and so confidence in this factor over soft X-ray energies is high. The experiment described above has shown that the theory for the Modified Fano Factor holds true for 1000 eV and 1487 eV photons and so this factor can be used to aid the development of future X-ray spectrometers, allowing EM-CCDs to be used effectively for the detection of low energy X-rays. The conditions under which an EM-CCD would be appropriate for use on a future X-ray spectrometer is discussed in [1].

VIII. Future work

With adequate cooling the CCD220 should be able to detect X-rays down to at least 200 eV, with the results providing further verification of the Modified Fano Factor. This will complete the study of this factor for soft X-rays. Currently the device's anti-reflection coating will hamper its low energy response, but this could be removed. It is expected that this factor will also hold at hard X-ray energies, but as these photon interactions generate a large number of e-h pairs through their interaction, the use of an EM-CCD to provide an improved SNR for low signal levels is not necessary.

Acknowledgements

I would like to thank e2v technologies for providing the devices used in the study, the team at the PTB beamline at BESSY II for their expertise, skill and professionalism in helping the data to be acquired, and David Burt and James Endicott of e2v and Mark Robbins of SSTL for technical advice.

References

[1] J. Tutt et al., "The Noise Performance of Electron Multiplying Charge-Coupled Devices at X-ray energies," IEEE Trans. Electrons Devices, Vol. 59 Issue 1 2011
[2] P. Jerram et al., "The LLLCCD: Low light imagining without the need for an intensifier," Proc. SPIE 4306, p.p 178-186, 2001.
[3] M. Robbins et al., "The Noise Performance of Electron Multiplying Charge-Coupled Devices," IEEE Trans. Electrons Devices, Vol. 50, No. 5, 2003.
[4] e2v CCD97 datasheet, A1A-CCD97BI-2P-IMO, Issue 3, 2004.
[5] e2v CCD220 provisional datasheet, CCD220BI Provisional, Issue B, 2007.
[6] M.J. Howes and D. V. Morgan, "Charge-Coupled Devices and systems," Wiley, 1979
[7] e2v private communication
[8] R. Reich et al.., "Integrated Electronic Shutter for Back-Illuminated Charge-Coupled Devices," IEEE Trans. Electrons Devices, Vol. 40, No. 7, 1993.
[9] D. Burt and J. Mason, "Simulations of a Back-illuminated CCD with Integrated Electronic Shutter," Laboratory working document 1993.
[10] J. Tutt et al., "A study of electron-multiplying CCDs for use on the International X-ray Observatory off-plane x-ray grating spectrometer," Proc. SPIE., Vol. 7742, 2010.
[11] G. Hopkinson et al., "Charge diffusion effect in CCD X-ray detectors. 1. Theory," Nuclear Instrument and Methods, Vol. 216, p.p 423-429 1983.

[12] J. Hiraga et al., "How Big Are Charge Clouds Inside the Charge-Coupled Device Produced by X-ray Photons," ISAS Research note, ISAS RN 656, 1998.
[13] C. R. Crowell, "Temperature dependence of Avalanche Multiplication in Semiconductors," Applied Physics Letters, Vol. 9, 1966.
[14] J.R. Janesick, "Photon transfer," SPIE Press, Bellingham, Washington, USA, p.p 34, 2007.
[15] R. Clarke, "CCD X-ray detectors: opportunities and challenges," Nuclear Instrument and Methods, Vol. 347 p.p 529-533, 1994.
[16] N. Meidinger et al., "Soft X-ray damage in CCD detectors," Nuclear Instrument and Methods, Vol. 439 p.p 319-336, 2000.
[17] R.C. Westhoff et al, "Low-Dark-Current, Back-Illuminated Charge-Coupled-devices," Proc. SPIE, Vol. 7249 2009.
[18] B.G. Magorrian and N.M. Allinson, "Particle and X-ray damage in pn-CCDs," Nuclear Instrument and Methods, p.p 599-604, 1988.
[19] G. Beutier et al., "Back-illuminated CCD for coherent soft X-ray imaging," Eur. Phys. J. Appl. Phys., Vol. 42 p.p 161-167, 2008.
[20] T.M.V. Bootsma et al., "Synchrotron calibration and response modelling of back-illuminated XMM-RGS CCDs," Nuclear Instrument and Methods, p.p 575-581, 2000.
[21] D.H. Lumb and G.R. Hopkinson., "Charge diffusion effect in CCD X-ray detectors II. Experimental results," Nuclear Instrument and Methods, Vol. 216 p.p 431-438, 1983.

BIOGRAPHIES

James Tutt James is a third year post-graduate student studying under Andrew Holland, Neil Murray and David Hall. James is working towards a PhD on detector developments for high resolution X-ray spectroscopy. This work involves the development and characterization of soft X-ray imaging spectrometers, based on both CCD and EM-CCD technology covering the 0.2-2 keV energy range.

Andrew Holland Andrew is an expert in detector physics and has worked on the development of a number of successful space instruments. Working on a range of detector developments over the past two decades, he has a wealth of knowledge and experience advising on instrument related issues, in particular radiation damage effects and the prediction of orbital performance.

Neil Murray Neil is an e2v funded PDRA in the centre for electronic imaging where he designs and builds a variety of experiments and techniques to perform detailed characterisation of CCDs in support of space missions. Neil also contributes with his technical expertise to the groups wider research interests and those of e2v technologies.

David Hall David is an e2v Research Fellow and has continued his research within the e2v centre for electronic imaging into the modelling of CCDs and novel imaging techniques, with particular interest in the development of innovative techniques and applications for the Electron-Multiplying CCD in synchrotron-based research and medical imaging.

Richard Harriss Richard is a second year post-graduate student working under Andrew Holland and Neil Murray. His thesis is based around looking at advanced CMOS imagers for scientific applications in particular providing a novel instrument for the UK Space Agencies first CubeSat mission.

Andrew Clarke Andrew is a post-graduate student, studying under Andrew Holland and David Hall. His research focuses on the 3D modelling of semiconductor detectors with model verification on test structures. Recent modelling has included the CCD204 and CCD273 to predict device functionality.

Anthony Evagora Anthony is a third year post-graduate student studying under Andrew Holland and Neil Murray. His thesis is focused on the ageing associated with Electron Multiplying CCDs. In addition to this he is also working on the effects of radiation damage and single event phenomena in the EM-CCD.